International Scientific Colloquium
Modelling for Material Processing
Riga, September 16-17, 2010

Liquid-Liquid Interface Instability in the Electro-Slag Remelting Process

A. Kharicha, A. Ludwig

Abstract

In the present paper a transient 2D model is used to explore the possible origin of the resistance fluctuation in the ESR process. The models couple efficiently the electric current distribution with the slag/gas and slag/metal pool interfaces. The procedure consists in simultaneously resolving the Navier-Stokes and the Maxwell equations.

Introduction

The Electro-Slag-Remelting (ESR) is an advanced technology for the production of components of e.g. high quality steels. Optimisation of the process efficiency and surface quality are directly linked with the electrode immersion depth. The best results are believed to be obtained with constant immersion depth and as shallow as possible. Nevertheless, the shallower immersion depth, the more difficult is to control the electric parameters (power, voltage). The extreme variations in voltage observed during such shallow immersion are attributed to the formation of air gap under the electrode, that can possibly lead to arcing and to deleterious oxidizing reactions. In opposite a too deep immersion depth is known to create poor surface and metallurgical quality in the final ingot. No system currently exists to measure the depth directly, so it must be inferred from measured parameters of the process. The variation of the resistance, known as resistance swing, is the mostly used method for the control of the electrode position [1]. However, the increase in resistance swing can be reliably, but not quantitatively, related with the immersion depth. In addition, it is known that the control currently used in industry can experience unexpected and unexplained difficulties, resulting in imperfections in the ingot being produced. This is why some efforts must be applied to the identification of process state, solely through analysis of electric process parameters. The aim of the present work is to compute numerically the time evolution of the resistance. To achieve this goal it is important to identify the phenomena that can generate these electric fluctuations. Assuming that most of the resistance is generated within the slag cap, our analysis will focus on the electric properties of this region. The slag region experiences strong flow turbulence that can induce locally strong temperature fluctuations. The electric conductivity of a typical slag is not constant, instead it increases with temperature. If the temperature at a point located within the slag fluctuates, the Joule released at this point fluctuates also. Recently, it was shown that these fluctuations have a considerable effect on the power generated in the slag [2]. A correction factor must be added to the joule heating source, especially in area with strong thermal turbulence, i.e. under the electrode and at the vicinity of the mould [2]. Nevertheless, the estimated standard deviation of the total resistance was found to not exceed 3 %. By modifying the chemical composition of the slag, the electrochemical reactions may modify the average electric conductivity. Large and fast fluctuations of the resistance can only be generated by modifying the shape of the slag cap. The shape of the electrode tip being melted represents the first boundary. The time scale associated with a shape modification is in the order of minutes (5-20 min), assuming a constant immersion depth it cannot induce fast resistance fluctuations. The solid slag that

develops at the mould (referred as slag skin) is a boundary that was considered for a long time as an electric insulator [3,4]. But recent experimental and numerical investigations have shown that typically 20% (but up to 80 %) of the total current can cross it to enter directly into the mould [2,5]. It is clear that a time fluctuation of the mould current intensity can induce a variation of the global resistance. The slag/ pool interface and the exposed slag surface are boundaries that are susceptible to move. Visual observations of the slag/air surface show a surface strongly affected by the slag eddies. Due to the presence of high temperatures, opacity of the materials, and the presence of the mould it is not possible to directly observe the behaviour the slag/pool interface. Although usually assumed flat, a previous work [6] using a Volume of fluid (VOF) model has shown that the interface between a layer of slag and steel layer in a cylindrical cavity is highly coupled with the distribution of the electric current. A full scale simulation of the ESR process using a VOF model has shown that the shape of the pool interface is likely to be non flat. Depending on whether a "flat" or "free" interface is assumed, an appreciable difference was found in the prediction of the pool shape and thickness [7]. This difference was due to a different magnitude and distribution of the Joule heat generated.

This work present the results given by 2D MHD model coupled with the phases distribution. The 2D model allows the movement of the electrode within the slag. The movements of the liquid interfaces are resolved in time and in space. Two different states are explored, one with shallow immersion depth, and a second with a deep penetration depth.

1. The Numerical Model

The axisymmetric calculation domain is presented in fig. 1. A rigid electrode is put in contact with a cylindrical container filled with a layer of liquid slag and an quantity of liquid steel. Most of properties of steel, slag and gas (N_2) are assumed to be constant. The electrode supplies a total 5Hz AC current of I_0=5000 Amperes. The influences of the melting, and of the falling droplets are not taken into account.

1.1. The VOF technique. In the VOF method the motion of the interface between immiscible liquids of different properties is governed by a phase indicator, the so-called volume fraction f, and an interface tracking method. The volume fraction f_k is equal to 0 outside of liquid k, and equal to 1 inside A standard advection equation governs the evolution of f_k for a given flow field $\vec{u}$:

$$\frac{Df}{Dt}=0 \quad \Rightarrow \quad \frac{\partial f}{\partial t}+\nabla\cdot(\vec{u}f)=0\,. \qquad (1)$$

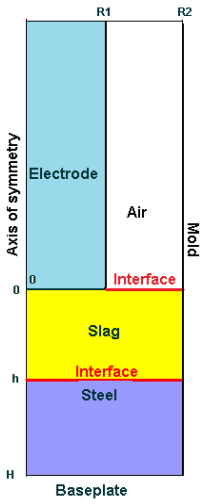

Fig. 1. Calculation domain

The local values of a physical property Θ (such as density, viscosity, electric conductivity) are interpolated by the following formula $\Theta=\Theta_1 f_1 + f_2\Theta_2 + f_3\Theta_3$, where the subscripts 1,2,3 indicate the corresponding phase. An explicit version of the VOF technique was used for the present calculations. The value of the surface tension is fixed to 1N/m at both interfaces [8]. Depending on the dynamic of the interfaces, the typical calculation time step lies in the range of 10^{-2}-10^{-4} second.

1.2. Fluid flow and heat transfer. The motion of the slag, gas, and liquid steel is computed with the buoyant Navier-Stokes equations. The effect of the turbulence is estimated with the help of the Realizable k-ε. The energy equation is solved in the fluid domain. The no-slip condition is applied at the electrode, the mould and the bottom boundary of the liquid pool. The temperature at the electrode/slag contact surface is fixed at the alloy liquidus temperature. The P1 radiation model is used to compute the radiation in the gas and slag media. This model is necessary in order to correctly estimate the heat radiation fluxes at the electrode, mould and

more important for any shape of the exposed slag surface. At the mould and at the bottom boundary, the temperature is fixed at the slag liquidus temperature. At the gas level, the radiative emissivity of the electrode and of the mould is taken equal to 0.8.

1.3. Electromagnetics. To solve the electromagnetic field, two techniques can be used, one based on the induced magnetic field $\vec{H}_\theta$, and another based on the electric potential *V*. Due to its simplicity, the method based induced magnetic field is the most widely used technique [2-7]. With no mould current, a single (or double in AC) equation must be solved with very simple boundary condition. When mould current is considered, the induction equation needs to be solved with the thin slag layer with enough grid point to correctly resolve the strong decrease in electric conductivity [2,5]. In the present work, the solid slag layer is modeled and not resolved [see next part]. The method based on the electric potential allows us to write the mould current in the simple form: $j_m = \sigma_w \frac{V}{\delta}$, (2)

where σ_w is the average electric conductivity within the slag skin, assumed to be 1000 times smaller than the conductivity of the slag at liquidus temperature. The potential at the mould and at the base plate is fixed to 0. The potential equation is computed from the equation of the conservation of the electric current: $\nabla \cdot \vec{j} = \vec{\nabla}(-\sigma\vec{\nabla}V) = 0$. The magnetic field is then extracted by solving the magnetic potential vector equations. Since the time resolution of the interface needs the use of very small time step, the choice is made here to resolve the oscillation of the imposed electric current (ω~5-50Hz). At the top of the electrode the following boundary simple DC condition is fixed:

$$-\sigma\frac{\partial V}{\partial z} = \frac{\sqrt{2}I_0}{\pi R_1^2}\sin(\omega t). \quad (3)$$

The Boundary condition at the mould consists in equalizing the electric flux to the mould current (2) when the adjacent cell is filled with slag, or to 0 in the other cases. Usually the Lorentz force and the Joule heat source are introduced in the corresponding equations only after time averaging [2-7]. In the present approach these sources are oscillating in time around their main values, allowing a full coupling between the hydrodynamic, the electromagnetic and the thermal phenomena.

1.4. Solid slag thickness Model. From the heat balance through the solid slag layer it is possible to extract a simple 1 D equation for the evolution of its thickness $\delta(z,t)$:

$$-\lambda\frac{\partial T}{\partial r} + \int_{R_e}^{R+\delta}\frac{j_m^2}{\sigma(T)}2\pi r dr - \rho C_p\left[\frac{\partial \bar{T}}{\partial t} + u_{melt}\frac{\partial \bar{T}}{\partial z}\right] - \rho L\left[\frac{\partial \delta}{\partial t} + u_{melt}\frac{\partial \delta}{\partial z}\right] = Q_{mould}. \quad (4)$$

The term from left to the right are the heat flux at the mould, the Joule heating in the solid layer, the convective transfer of energy, and the latent heat of fusion released during variation in thickness of δ. The effect of the elevation of the slag level during the melting is taken into account through the velocity u_{melt}, related to the meltrate (2kg/min). This approach allows also the slag skin thickness to vary with the meltrate, the higher the melting rate, the thinner the slag skin.

The heat flux at the slag skin/mould is estimated with a heat transfer coefficient *H*:

$$Q_{mould} = H(T_{mould} - T_{water}) = \lambda\frac{T_{Liquidus} - T_{mould}}{\delta}, \quad \text{and } \bar{T} = \frac{T_{Liquidus} + T_{mould}}{2}. \quad (5)$$

Eq. 4 and Eq. 5 are solved iteratively to get both the new slag thickness and the temperature at slag skin/mould interface ($T_{mould} \sim 350 - 550K$). In the present calculation the Joule heating source is simplified by using the average slag skin electric conductivity:

$$\int_{R_2}^{R_2+\delta} \frac{j_m^2}{\sigma(T)} dr = \frac{j_m^2}{\sigma_w} \delta \,. \tag{6}$$

In the next iteration the mould current is recomputed from the given slag thickness. Without the presence of mould current, the solid slag thickness is only controlled by the magnitude of the heat flux at the mould. By adding a heat source within the slag skin, the presence of mould currents decreases this thickness, which in turn increases the quantity of mould current (2). This cycle of increases is stopped when the electric current has found the pattern that minimizes the global resistance. This simple approach can model the creation of the slag skin at the level of the exposed slag surface where time oscillations are expected. After having computed the electric currents pattern, the total electric resistance include the resistance of the liquid slag (volume integral) and of the slag skin (integrated over the slag height):

$$Res(t) = \frac{1}{I_0^2} \left(\int \frac{j^2(r,z,t)}{\sigma(T,t)} dv + \int \frac{j_m^2(z,t)}{\sigma_w} dz \right). \tag{7}$$

2. Application of the model

2.1. Shallow immersion depth: 0 and 4 mm. In the case when the electrode is just put in contact with the slag surface, the simulation shows a strongly fluctuating slag/gas interface (Fig. 2&5). During the calculations, the electric current intensity was progressively increased. Far before reaching the desired intensity, at about 1400 Amps, a large gas bubble was created between the electrode and the slag media (Fig. 2). During the insertion of the gas, the electric current lines are shifted towards the electrode centre, this phenomena is at the origin of the strong increase of the resistance (Fig. 3 B). The strong decrease of resistance at the stage C is due to occurrence of a small surface contact between the slag and the electrode. Due to some flow turbulence, the electric contact is very unstable. Combined with hazardous electric contacts, the forward movement of the gas gap led to a new increase in resistance (Fig.3 stage D).

In order to avoid such gap, we increased the immersion depth to 4 mm. Now, the evolution of the resistance with time in figure 4 can be qualified as normal (swing~18 %). There are the presence of fast (~1-20 Hz) and slow fluctuations (~10^{-3}-10^{-1} Hz). The fast are due to interfaces movements, the slowest frequencies are due to the evolution of the slag temperature. It can be noticed that negative picks are more numerous than positive. Figure 5 shows the interface configurations that lead to positive and negative picks. The key mechanism is the coupling between the quantity of mould current and the dynamic of the slag/gas interface. Although always present, the quantity of the mould current increases dramatically when the level of the slag/gas interface at the mould reaches levels where the solid slag layer is not yet (or being) developed (Fig. 10). The resistance is then at its smallest level especially if the level of slag is also high at the electrode (Fig. 5 a). When the interface is at its lowest mould point, the presence of the developed slag skin will force most of the electric current lines to be redirected towards the pool (Fig.5 b). This situation will lead to a strong increase of the resistance. In the present simulations the occurrence of negative picks seems to be higher than the occurrence of the positive picks. The distribution of the Lorentz force shows that both configurations in figure 5 are unstable. Nevertheless, the density of electric current is higher under the interface when the slag/gas interface is convex (low resistance). Under the action of this non-uniform force, the interface will increase its curvature until equilibrium with static pressure is reached. In the case of concave slag/gas interface, the highest electric current density is located at the vicinity of the electrode. If the Lorentz force acting on the interface is not stopped by the surface tension, the contact surface between the electrode and the slag will diminish, opening the possibility of gas gap

occurrence. It is then obvious that the ratio between the intensity of the picks depends on the fill ratio. A higher slag height will produce higher positive picks, while a smaller electrode-mould distance will induce lower negative picks.

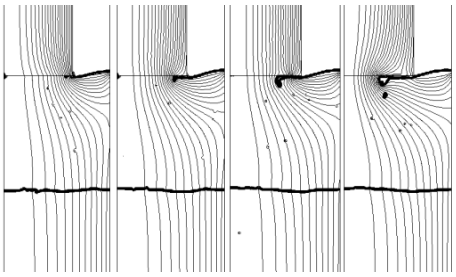

Fig. 2: Electric current lines during the formation of an air gap between the slag and the electrode (see also figure 3)

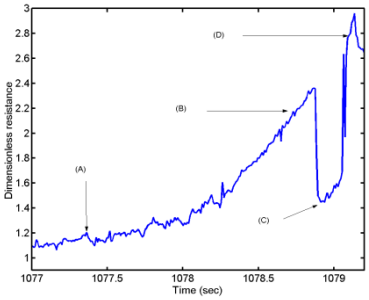

Fig. 3: Evolution of the resistance during the formation of an air gap under the electrode

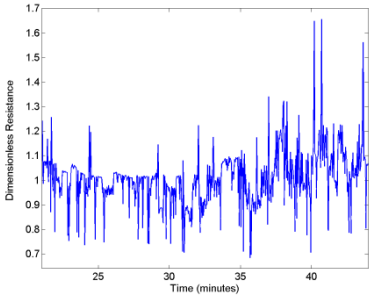

Fig. 4: Resistance swing for 5 mm penetration depth

2.2. Immersion depth of 50 mm. The electrode is moved downward at a speed of 1.8 mm/s from the previous 4 mm depth (averaged) until reaching a shift of about 30 mm, corresponding to 50 mm electrode immersion depth. This speed, is relatively small compared to the maximum velocity calculated (~20 mm/s). During the electrode drive, the main resistance decreases dramatically (Figure 6). In opposite to the slag/pool interface, the slag/gas interface does not seem to be affected by the electrode movement (Figure 7). During the first 10 minutes, the elevation of the slag surface increases the surface through which the electric current enters the mould. Although the electrode is now closer to the liquid pool, the average proportion of mould current increased from 30 to 50 %. After 20 seconds, the calculations show an increase of the average resistance with time, it is due to the slow formation of the solid slag thickness and to the redirection of the electric current lines towards the liquid pool. After 10 minutes, a "steady state" regime is reached in which the main source of the resistance swing is the oscillation of the liquid pool interface (Fig. 8). Due to the low magnitude of mould current, and to a weak slag/gas interface movement, negative picks are absent from the time evolution of the resistance (Fig. 9). The maximum amplitude of the interface slag/pool movement is about 2 cm, with main frequencies in the 1-30 Hz range. The picks are only 30 % higher than the average value; the corresponding resistance swing is lower than 4 %. The computed solid slag thickness (Fig. 10) is larger than in the previous case, except at the level of the electrode. This behaviour can be explained by a lower bulk temperature usually associated with deep electrode penetration depth. The thinner layer observed at the level of the electrode is due to the presence of mould current and to flow convection (Fig. 8).

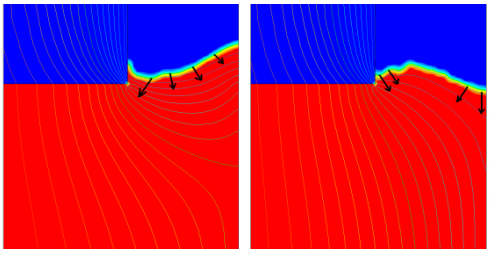

Fig. 5: Zoom over the exposed slag surface. Lorentz force directions are marked in black

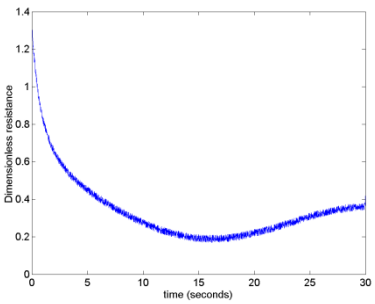

Fig. 6: Average resistance during the electrode penetration into the slag

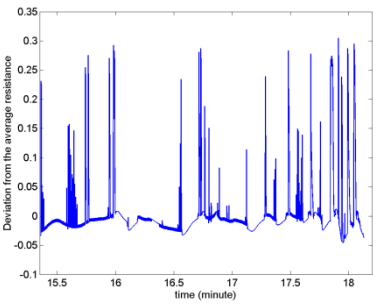

Fig. 9: Typical resistance swing during steady state (50mm penetration depth)

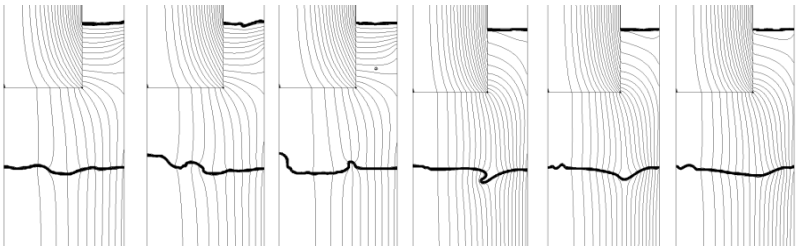

Fig. 7: Electric current lines and interface positions at 15 seconds after end of electrode movement

Fig. 8: Three successive MHD configurations during steady state

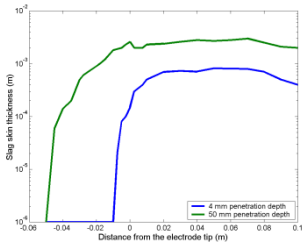

Fig. 10: Evolution of the solid slag thickness along the mould wall during steady state.

Conclusion

ESR process is inherently a dynamic process. Analysis of time data of the resistance has the potential to expose a number of abnormal or undesired process attributes (arcing, too deep electrode penetration depth). In order to improve process diagnostics, the identification of these attributes remained an area of interest for a number of years. The increasing capability of computational power has opened the possibility to explore with CFD techniques complex coupled phenomena. A numerical model was built with good ability to handle free surfaces, and good flexibility to handle the dynamic electromagnetic fields. The model was applied to a small ESR process to explore the interaction between the interfaces and the quantity of mould current. The time evolution of the resistance was recorder for each simulation run. The strong coupling between the slag/pool, slag/air interfaces, and mould current gives a new insight into the nature of the MHD oscillation present in the ESR process. This work should be taken as a first tentative exploration of the potential to incorporate control action based on the linkage between the physical process and the fluctuations associated with the resistance signal.

However in the real process, these fluctuations are likely to be three dimensional. In addition several important phenomena were not taking account, such as the evolution of the electrode shape and the effect of the droplets flow. Although numerical requirements for 3D MHD flows with free interfaces are considerable, the building of a 3D model of the ESR process is being planned.

References

[1] D.K. Melgaard, R.L. Williamson, and J. J beaman. JOM, 1998 March, p13-17.
[2] A. Kharicha, W. Schützenhöfer, A. Ludwig, R. Tanzer. W. Int. J. Cast Metals Research, 2008, in press.
[3] B. Hernandez-Morales and A. Mitchell, Ironmaking & Steelmaking, Vol. 26 No. 6 (1999), p.423-438.
[4] V.WEBER, A. JARDY et al. Metall Mater Trans.B. 14 january 2009.
[5] A. Kharicha, W. Schützenhöfer, A. Ludwig, R. Tanzer. Steel Research International. Vol.79 (8), 2008, p 632-636.
[6] A. Kharicha, A. Ludwig and M. Wu. Materials Science & Engineering A, 413-414 (2005) p. 129-134.
[7] A. Kharicha, W. Schützenhöfer, A. Ludwig and G. Reiter. Modeling of Casting, Welding and Advanced Solidification Processes XI Opio, France (June 2006).
[8] H.Sun, K.Nakashima and K.Mori, ISIJ international, Vol. 46 (2006), No.3, pp. 407-412.

Authors

Dr. Kharicha, Abdellah
Ludwig, A.
University of Leoben,
Franz-Joseph strasse, 8.
8700 Leoben, AUSTRIA
Abdellah.kharicha@notes.unileoben.ac.at